Research Article

Douglas R. Q. Pacheco and Olaf Steinbach*

Optimal Pressure Recovery Using an Ultra-Weak Finite Element Method for the Pressure Poisson Equation and a Least-Squares Approach for the Gradient Equation

https://doi.org/10.1515/cmam-2021-0242
Received December 21, 2021; revised October 13, 2023; accepted October 18, 2023

Abstract: Reconstructing the pressure from given flow velocities is a task arising in various applications, and the standard approach uses the Navier–Stokes equations to derive a Poisson problem for the pressure p. That method, however, artificially increases the regularity requirements on both solution and data. In this context, we propose and analyze two alternative techniques to determine $p \in L^2(\Omega)$. The first is an ultra-weak variational formulation applying integration by parts to shift all derivatives to the test functions. We present conforming finite element discretizations and prove optimal convergence of the resulting Galerkin–Petrov method. The second approach is a least-squares method for the original gradient equation, reformulated and solved as an artificial Stokes system. To simplify the incorporation of the given velocity within the right-hand side, we assume in the derivations that the velocity field is solenoidal. Yet this assumption is not restrictive, as we can use non-divergence-free approximations and even compressible velocities. Numerical experiments confirm the optimal a priori error estimates for both methods considered.

Keywords: Pressure Poisson Equation, Ultra-Weak Variational Formulation, Least-Squares Approach

MSC 2020: 65N30

1 Introduction

In fluid systems, using the velocity field to compute the pressure is a task with established relevance for both theory and applications. For example, this can be used in fractional-step solvers to update the pressure from a previously computed velocity [11], or in clinical practice to estimate arterial pressure from imaging-based velocity measurements [15]. The most popular approach to solve this inverse problem is the so-called pressure Poisson equation (PPE) obtained from the divergence of the Navier–Stokes momentum equation. Of course, applying the divergence increases the regularity requirements on both the unknown pressure p and the given velocity $\boldsymbol{u}$, imposing numerical challenges. In fact, standard (weak) variational formulations for the PPE require continuous pressure and smooth velocities for conformity, which poses practical limitations [4, 13]. In this context, we introduce here an ultra-weak (often called *very weak* [3, 6]) variational formulation for the PPE, and conforming finite element methods for its discretization. The first and perhaps only time an ultra-weak formulation has been mentioned – yet not analyzed nor discretized – for the PPE was in an article on pressure boundary conditions [17]. Apart from that, ultra-weak formulations are normally either used for merely first-

***Corresponding author: Olaf Steinbach,** Institut für Angewandte Mathematik, TU Graz, Graz, Austria, e-mail: o.steinbach@tugraz.at
Douglas R. Q. Pacheco, Department of Mathematical Sciences, Norwegian University of Science and Technology, Trondheim, Norway, e-mail: douglas.pacheco@alumni.usp.br

order boundary value problems [8] (where standard Lagrangian finite element spaces can be used), or handled as a mixed system to circumvent smoothness requirements on the test space [3]. Our idea, on the other hand, is to work with more regular test functions, which allows us to stay with a standard L^2 requirement for the pressure. A rare example of such a type of discretization is a recent work on hyperbolic problems [10].

Alternatively to the ultra-weak framework, we also discuss a least-squares approach to find $p \in L^2(\Omega)$ without deriving a Poisson problem, i.e., considering the original gradient equation for the pressure. The idea is to construct an operator equation that is realized by solving an artificial Stokes problem. Both approaches considered here require the same regularity on the pressure, but are analyzed and realized in very different ways.

On a domain $\Omega \subset \mathbb{R}^n$, $n = 2$ or 3, with Lipschitz boundary $\Gamma = \partial\Omega$, the model problem considers the momentum equation

$$\nabla p = \boldsymbol{f} + \nu \Delta \boldsymbol{u} \quad \text{in } \Omega, \tag{1.1}$$

where $\boldsymbol{u}$ is a given velocity field, ν is the fluid viscosity, and $\boldsymbol{f}$ is a given vector. This can be seen as a general flow setting, since $\boldsymbol{f}$ can include not only external forces, but also velocity-dependent terms stemming from the flow equations (e.g., convection or acceleration terms). Moreover, most applications consider an incompressible flow, that is,

$$\operatorname{div} \boldsymbol{u} = 0 \quad \text{in } \Omega. \tag{1.2}$$

Here we will use (1.2) to simplify the evaluation of the vector Laplacian in (1.1). Afterwards we can use non-divergence-free (finite element) approximations of the velocity, or even consider compressible velocities from the beginning (with an appropriate form of the viscous term).

The pressure recovery problem considers $\boldsymbol{u}$ as given, so we do not seek to solve the system composed of (1.1) and (1.2); instead, we wish to use those equations to find the pressure p. Yet, since (1.1) is vector-valued and p is a scalar, we get an overdetermined system when applying standard discretization schemes. This motivates using least-squares approaches.

2 The Pressure Poisson Equation

2.1 Weak Formulation

The classical technique to find p is the pressure Poisson equation. Although it can be set up by deriving a Poisson equation for p, an equivalent formulation is to minimize the quadratic functional

$$\mathcal{J}(p) = \frac{1}{2} \| \nabla p - \boldsymbol{f} - \nu \Delta \boldsymbol{u} \|^2_{L^2(\Omega)}. \tag{2.1}$$

Its minimizer is found as the solution $p \in H^1(\Omega)$ of the variational formulation

$$\int_\Omega \nabla p \cdot \nabla q \, dx = \int_\Omega (\boldsymbol{f} + \nu \Delta \boldsymbol{u}) \cdot \nabla q \, dx \quad \text{for all } q \in H^1(\Omega). \tag{2.2}$$

The pressure p is only unique up to an additive constant, hence we use the scaling condition $p \in L^2_0(\Omega)$, that is, $p \in L^2(\Omega)$ satisfying

$$\int_\Omega p \, dx = 0. \tag{2.3}$$

While standard variational formulations for flow problems consider $(\boldsymbol{u}, p) \in \boldsymbol{H}^1(\Omega) \times L^2(\Omega)$, formulation (2.2) requires more regularity, i.e., $(\boldsymbol{u}, p) \in \boldsymbol{H}^2(\Omega) \times H^1(\Omega)$. This restricts the possibilities for discretizing the solution p and the data $\boldsymbol{u}$. In biomedical applications, for example, the velocity $\boldsymbol{u}$ is often a first-order interpolation of imaging data, in which case the vector Laplacian in (2.2) cannot be approximated [4]. Even if we had only first-order terms, e.g., $(\nabla \boldsymbol{u})\boldsymbol{u}$ as in an Euler flow, the fact that $\boldsymbol{u}$ is a piecewise linear interpolation limits the pressure convergence to linear, regardless of the polynomial order used for p_h (see [1]). Motivated by these limitations of the weak PPE, we propose an ultra-weak formulation that allows piecewise constant approximations for the pressure and less regular data.

Note 1: Red parts indicate major changes. Please check them carefully.

2.2 Ultra-Weak Variational Formulation

The idea is to replace $q \in H^1(\Omega)$ in (2.2) with more regular test functions φ. This allows applying integration by parts, giving us

$$\int_\Gamma p\partial_n\varphi\, ds_x + \int_\Omega p[-\Delta\varphi]\, dx = \int_\Omega (\boldsymbol{f} + \nu\Delta\boldsymbol{u})\cdot\nabla\varphi\, dx.$$

Requesting $\partial_n\varphi = 0$ on Γ yields

$$\int_\Omega p[-\Delta\varphi]\, dx = \int_\Omega (\boldsymbol{f} + \nu\Delta\boldsymbol{u})\cdot\nabla\varphi\, dx. \tag{2.4}$$

For the velocity term, we use (1.2) and integration by parts to write

$$\begin{aligned}
\int_\Omega \Delta\boldsymbol{u}\cdot\nabla\varphi\, dx &= \int_\Omega [\nabla(\operatorname{div}\boldsymbol{u}) - \operatorname{curl}(\operatorname{curl}\boldsymbol{u})]\cdot\nabla\varphi\, dx \\
&= -\int_\Omega [\operatorname{curl}(\operatorname{curl}\boldsymbol{u})]\cdot\nabla\varphi\, dx \\
&= \int_\Gamma [\operatorname{curl}\boldsymbol{u}]\cdot(\boldsymbol{n}_x\times\nabla\varphi)\, ds_x - \int_\Omega [\operatorname{curl}\boldsymbol{u}]\cdot[\operatorname{curl}(\nabla q)]\, dx \\
&= \int_\Gamma (\operatorname{curl}\boldsymbol{u})\cdot(\boldsymbol{n}_x\times\nabla\varphi)\, ds_x,
\end{aligned}$$

which holds for both $n = 2$ and $n = 3$, with the appropriate definitions of the curl and the cross product. Note that in the above derivation we consider the exact solenoidal velocity, which later on can be replaced by a non-divergence-free approximation. Finally, we include the zero mean pressure condition and obtain an extended variational formulation: find $p \in X := L^2(\Omega)$ such that

$$\int_\Omega p[-\Delta\varphi]\, dx + \frac{1}{|\Omega|}\int_\Omega p\, dx \int_\Omega \varphi\, dx = \int_\Omega \boldsymbol{f}\cdot\nabla\varphi\, dx + \int_\Gamma (\nu\operatorname{curl}\boldsymbol{u})\cdot(\boldsymbol{n}_x\times\nabla\varphi)\, ds_x \tag{2.5}$$

is satisfied for all $\varphi \in Y := \{\varphi \in H^1_\Delta(\Omega) : \partial_n\varphi = 0 \text{ on } \Gamma\}$, where

$$H^1_\Delta(\Omega) := \{\varphi \in H^1(\Omega) : \Delta\varphi \in L^2(\Omega)\}, \quad |\Omega| := \int_\Omega dx.$$

Unique solvability of the ultra-weak variational formulation (2.5) is based on an inf-sup stability condition for the bilinear form

$$a(p,\varphi) := \int_\Omega p[-\Delta\varphi]\, dx + \frac{1}{|\Omega|}\int_\Omega p\, dx \int_\Omega \varphi\, dx, \quad p \in X,\ \varphi \in Y.$$

While the norm for $p \in X = L^2(\Omega)$ is obvious, for $\varphi \in H^1(\Omega)$ an equivalent norm is

$$\|\varphi\|^2_{H^1(\Omega),\Omega} := \|\nabla\varphi\|^2_{L^2(\Omega)} + \frac{1}{|\Omega|}\left(\int_\Omega \varphi\, dx\right)^2.$$

For $\varphi \in H^1_\Delta(\Omega)$ we therefore define the norm

$$\|\varphi\|^2_{H^1_\Delta(\Omega)} := \|\nabla\varphi\|^2_{L^2(\Omega)} + \frac{1}{|\Omega|}\left(\int_\Omega \varphi\, dx\right)^2 + \|\Delta\varphi\|^2_{L^2(\Omega)}.$$

At this time we recall Poincaré's inequality: for all $u \in H^1(\Omega)$, there holds

$$\int_\Omega [u - u_\Omega]^2\, dx \le c_P \int_\Omega |\nabla u|^2\, dx, \quad u_\Omega = \frac{1}{|\Omega|}\int_\Omega u\, dx, \tag{2.6}$$

which is equivalent to

$$\int_\Omega u^2\, dx \le \frac{1}{|\Omega|}\left(\int_\Omega u\, dx\right)^2 + c_P \int_\Omega |\nabla u|^2\, dx. \tag{2.7}$$

Now we are in a position to state an equivalent norm in $Y \subset H^1_\Delta(\Omega)$, namely,

$$\|\varphi\|_Y^2 := \|\Delta\varphi\|^2_{L^2(\Omega)} + \frac{1}{|\Omega|}\left(\int_\Omega \varphi(x)\,dx\right)^2.$$

Lemma 2.1. *The norm $\|\varphi\|_Y$ defines an equivalent norm in $Y \subset H^1_\Delta$, i.e., there hold the norm equivalence inequalities*

$$\frac{1}{\max\{1 + c_P, 1 + c_P{}^{-1}\}}\|\varphi\|^2_{H^1_\Delta(\Omega)} \le \|\varphi\|_Y^2 \le \|\varphi\|^2_{H^1_\Delta(\Omega)} \quad \text{for all } \varphi \in Y.$$

Proof. While the upper estimate is trivial, it remains to prove the lower bound. For $\varphi \in Y$ we have, when applying Green's first formula and using $\partial_n\varphi = 0$ on Γ,

$$\begin{aligned}\|\nabla\varphi\|^2_{L^2(\Omega)} &= \int_\Omega \nabla\varphi\cdot\nabla\varphi\,dx = \int_\Gamma \varphi\partial_n\varphi\,ds_x + \int_\Omega [-\Delta\varphi]\varphi\,dx \\ &= \int_\Omega [-\Delta\varphi]\varphi\,dx \le \|\Delta\varphi\|_{L^2(\Omega)}\|\varphi\|_{L^2(\Omega)}.\end{aligned}$$

Now, using Young's inequality for some $\gamma > 0$ and the Poincaré inequality (2.7), this gives

$$\begin{aligned}\|\nabla\varphi\|^2_{L^2(\Omega)} &\le \|\Delta\varphi\|_{L^2(\Omega)}\|\varphi\|_{L^2(\Omega)} \le \frac{1}{2}\gamma\|\Delta\varphi\|^2_{L^2(\Omega)} + \frac{1}{2\gamma}\|\varphi\|^2_{L^2(\Omega)} \\ &\le \frac{1}{2}\gamma\|\Delta\varphi\|^2_{L^2(\Omega)} + \frac{1}{2\gamma}\left[\frac{1}{|\Omega|}\left(\int_\Omega \varphi\,dx\right)^2 + c_P\int_\Omega |\nabla\varphi|^2\,dx\right].\end{aligned}$$

In particular, taking $\gamma = c_P$ results in

$$\|\nabla\varphi\|^2_{L^2(\Omega)} \le c_P\|\Delta\varphi\|^2_{L^2(\Omega)} + \frac{1}{c_P|\Omega|}\left(\int_\Omega \varphi\,dx\right)^2,$$

and hence

$$\begin{aligned}\|\varphi\|^2_{H^1_\Delta(\Omega)} &= \|\nabla\varphi\|^2_{L^2(\Omega)} + \frac{1}{|\Omega|}\left(\int_\Omega \varphi\,dx\right)^2 + \|\Delta\varphi\|^2_{L^2(\Omega)} \\ &\le \left(1 + \frac{1}{c_P}\right)\frac{1}{|\Omega|}\left(\int_\Omega \varphi\,dx\right)^2 + \left(1 + c_P\right)\|\Delta\varphi\|^2_{L^2(\Omega)} \\ &\le \max\left\{1 + c_P, 1 + \frac{1}{c_P}\right\}\left[\frac{1}{|\Omega|}\left(\int_\Omega \varphi\,dx\right)^2 + \|\Delta\varphi\|^2_{L^2(\Omega)}\right]\end{aligned}$$

follows. □

For $(p,\varphi) \in X \times Y$ we now have, using Hölder's inequality,

$$\begin{aligned}a(p,\varphi) &= \int_\Omega p[-\Delta\varphi]dx + \frac{1}{|\Omega|}\int_\Omega p\,dx\int_\Omega \varphi\,dx \\ &\le \|p\|_{L^2(\Omega)}\|\Delta\varphi\|_{L^2(\Omega)} + \frac{1}{|\Omega|}\int_\Omega p\,dx\int_\Omega \varphi\,dx \\ &\le \left[\|p\|^2_{L^2(\Omega)} + \frac{1}{|\Omega|}\left(\int_\Omega p\,dx\right)^2\right]^{\frac{1}{2}}\left[\|\Delta\varphi\|^2_{L^2(\Omega)} + \frac{1}{|\Omega|}\left(\int_\Omega \varphi\,dx\right)^2\right]^{\frac{1}{2}} \\ &\le \sqrt{2}\|p\|_{L^2(\Omega)}\|\varphi\|_Y, \qquad (2.8)\end{aligned}$$

that is, boundedness. We can now state unique solvability of the variational problem (2.5).

Theorem 2.2. *Let* $(\boldsymbol{u}, p) \in \boldsymbol{H}^1(\Omega) \times L^2_0(\Omega)$ *satisfy* (1.1) *and* (1.2). *Then the pressure* $p \in L^2(\Omega)$ *is given as the unique solution of the extended variational formulation* (2.5), *which satisfies the scaling condition* (2.3), *that is,* $p \in L^2_0(\Omega)$.

Proof. For $p \in L^2(\Omega)$ we consider the splitting

$$p(x) = p_0(x) + \varrho, \quad \varrho = \frac{1}{|\Omega|} \int_\Omega p \, dx, \quad \int_\Omega p_0 \, dx = 0,$$

where we have

$$\|p\|^2_{L^2(\Omega)} = \int_\Omega p^2 \, dx = \int_\Omega [p_0(x) + \varrho]^2 \, dx = \int_\Omega [p_0(x)]^2 \, dx + 2\varrho \int_\Omega p_0 \, dx + |\Omega| \varrho^2,$$

that is,

$$\|p\|^2_{L^2(\Omega)} = \|p_0\|^2_{L^2(\Omega)} + \frac{1}{|\Omega|} \left(\int_\Omega p \, dx \right)^2.$$

Let $\varphi \in H^1(\Omega)$ be the unique weak solution of the Neumann boundary value problem

$$-\Delta \varphi = p_0 \quad \text{in } \Omega, \quad \partial_n \varphi = 0 \quad \text{on } \Gamma, \quad \int_\Omega \varphi \, dx = \int_\Omega p \, dx.$$

Then

$$\begin{aligned} a(p, \varphi) &= \int_\Omega p[-\Delta \varphi] \, dx + \frac{1}{|\Omega|} \int_\Omega p \, dx \int_\Omega \varphi \, dx \\ &= \int_\Omega [p_0 + \varrho] p_0 \, dx + \frac{1}{|\Omega|} \left(\int_\Omega p \, dx \right)^2 \\ &= \int_\Omega [p_0]^2 \, dx + \frac{1}{|\Omega|} \left(\int_\Omega p \, dx \right)^2 = \|p\|^2_{L^2(\Omega)} \\ &= \int_\Omega [-\Delta \varphi]^2 \, dx + \frac{1}{|\Omega|} \left(\int_\Omega \varphi \, dx \right)^2 = \|\varphi\|^2_Y \end{aligned}$$

implies

$$a(p, \varphi) = \|p\|_{L^2(\Omega)} \|\varphi\|_Y,$$

and therefore the inf-sup condition

$$\|p\|_{L^2(\Omega)} \le \sup_{0 \neq \varphi \in Y} \frac{a(p, \varphi)}{\|\varphi\|_Y} \quad \text{for all } p \in L^2(\Omega) \tag{2.9}$$

follows. On the other hand, for $0 \neq \varphi \in Y \subset H^1_\Delta(\Omega)$ we first compute

$$\alpha = \frac{1}{|\Omega|} \int_\Omega \varphi \, dx,$$

then define $p = -\Delta \varphi + \alpha \in L^2(\Omega)$. For this particular choice we obtain

$$\begin{aligned} a(p, \varphi) &= \int_\Omega p[-\Delta \varphi] \, dx + \frac{1}{|\Omega|} \int_\Omega p \, dx \int_\Omega \varphi \, dx \\ &= \int_\Omega [-\Delta \varphi + \alpha][-\Delta \varphi] \, dx + \frac{1}{|\Omega|} \int_\Omega [-\Delta \varphi + \alpha] \, dx \int_\Omega \varphi \, dx \\ &= \int_\Omega [\Delta \varphi]^2 \, dx + \frac{1}{|\Omega|} \left(\int_\Omega \varphi dx \right)^2 \\ &= \|\varphi\|^2_Y > 0, \end{aligned}$$

where we have used

$$\int_\Omega \Delta\varphi \, dx = \int_\Gamma \partial_n \varphi_x \, ds_x = 0 \quad \text{for } \varphi \in Y.$$

Hence, we have that all assumptions of the Babuška–Brezzi theorem are satisfied, see, e.g., [7], and therefore unique solvability of (2.5) follows. In particular, for $\varphi \equiv 1$ we finally conclude the scaling condition (2.3). □

2.3 Ultra-Weak Finite Element Methods

Let $X_h = \text{span}\{\psi_k\}_{k=1}^N \subset X = L^2(\Omega)$ be the space of piecewise constant basis functions ψ_k defined with respect to some admissible decomposition of Ω into finite elements τ_k of local mesh size h_k, and with global mesh size $h = \max_{k=1,\dots,N} h_k$. For simplicity we assume that the mesh is globally quasi-uniform, that is, $h_k \sim h$ for all $k = 1, \dots, N$. Then the finite element variational formulation of (2.5) is to find $p_h \in X_h$ such that

$$\int_\Omega p_h[-\Delta\varphi_h] \, dx + \frac{1}{|\Omega|} \int_\Omega p_h \, dx \int_\Omega \varphi_h \, dx = \int_\Omega \boldsymbol{f} \cdot \nabla\varphi_h \, dx + \int_\Gamma (\nu \operatorname{curl} \boldsymbol{u}) \cdot (\boldsymbol{n}_x \times \nabla\varphi_h) \, ds_x \tag{2.10}$$

is satisfied for all $\varphi_h \in Y_h$, where the finite element space $Y_h \subset Y$ remains to be specified. At this time we assume $\dim Y_h = \dim X_h$ and the discrete inf-sup or Babuška–Brezzi–Ladyshenskaya condition

$$c_S \|p_h\|_{L^2(\Omega)} \le \sup_{0 \neq \varphi_h \in Y_h} \frac{a(p_h, \varphi_h)}{\|\varphi_h\|_Y} \quad \text{for all } p_h \in X_h. \tag{2.11}$$

Using standard arguments, see, e.g., [7], we conclude unique solvability of the Galerkin–Petrov scheme (2.10), as well as Cea's lemma

$$\|p - p_h\|_{L^2(\Omega)} \le c \inf_{q_h \in X_h} \|p - q_h\|_{L^2(\Omega)}, \tag{2.12}$$

and hence the a priori error estimate

$$\|p - p_h\|_{L^2(\Omega)} \le c h^s |p|_{H^s(\Omega)} \tag{2.13}$$

when assuming $p \in H^s(\Omega)$ for some $s \in [0, 1]$. In particular, for $p \in H^1(\Omega)$ we obtain linear convergence for a piecewise constant approximation p_h.

It remains to define a suitable test space $Y_h = \text{span}\{\varphi_k\}_{k=1}^N \subset Y$ such that the discrete stability condition (2.11) is satisfied. For a given $\varphi_h \in Y_h$ we define $\overline{p}_h = Q_h[-\Delta\varphi_h] \in X_h$ as the piecewise constant L^2 projection satisfying

$$\int_\Omega \overline{p}_h q_h \, dx = \int_\Omega [-\Delta\varphi_h] q_h \, dx \quad \text{for all } q_h \in X_h. \tag{2.14}$$

In particular, for $q_h \equiv 1 \in X_h$ this gives

$$\int_\Omega \overline{p}_h \, dx = \int_\Omega [-\Delta\varphi_h] \, dx = -\int_\Gamma \partial_n \varphi_h \, ds_x = 0.$$

From (2.14) we immediately conclude the stability estimate

$$\|\overline{p}_h\|_{L^2(\Omega)} \le \|\Delta\varphi_h\|_{L^2(\Omega)},$$

which holds for any choice of the finite element test space Y_h. We now assume that Y_h is chosen in such a way that also the reverse inequality

$$\|\overline{p}_h\|_{L^2(\Omega)} \ge c_{Y_h} \|\Delta\varphi_h\|_{L^2(\Omega)} \tag{2.15}$$

is satisfied for a positive constant $c_{Y_h} \le 1$. Possible choices will be discussed at the end of this section.

We now define

$$p_h(x) = \overline{p}_h(x) + \alpha \in X_h, \quad \alpha = \frac{1}{|\Omega|} \int_\Omega \varphi_h \, dx,$$

which also implies

$$\alpha = \frac{1}{|\Omega|} \int_\Omega p_h \, dx, \quad \int_\Omega p_h \, dx = \int_\Omega \varphi_h \, dx.$$

With this we compute, using (2.15),

$$\begin{aligned}
a(p_h,\varphi_h) &= \int_\Omega p_h[-\Delta\varphi_h]\,dx + \frac{1}{|\Omega|}\int_\Omega p_h\,dx\int_\Omega \varphi_h\,dx \\
&= \int_\Omega \overline{p}_h[-\Delta\varphi_h]\,dx + \frac{1}{|\Omega|}\int_\Omega p_h\,dx\int_\Omega \varphi_h\,dx \\
&= \int_\Omega [\overline{p}_h]^2\,dx + \frac{1}{|\Omega|}\left(\int_\Omega p_h\,dx\right)^2 \\
&= \left[\|\overline{p}_h\|^2_{L^2(\Omega)} + \frac{1}{|\Omega|}\left(\int_\Omega p_h\,dx\right)^2\right]^{\frac12}\left[\|\overline{p}_h\|^2_{L^2(\Omega)} + \frac{1}{|\Omega|}\left(\int_\Omega p_h\,dx\right)^2\right]^{\frac12} \\
&\geq c_{Y_h}\left[\|\Delta\varphi_h\|^2_{L^2(\Omega)} + \frac{1}{|\Omega|}\left(\int_\Omega \varphi_h\,dx\right)^2\right]^{\frac12}\left[\|\overline{p}_h\|^2_{L^2(\Omega)} + \frac{1}{|\Omega|}\left(\int_\Omega p_h\,dx\right)^2\right]^{\frac12} \\
&= c_{Y_h}\|\varphi_h\|_Y\|p_h\|_{L^2(\Omega)},
\end{aligned}$$

which implies the stability condition

$$c_{Y_h}\|\varphi_h\|_Y \leq \sup_{0\neq q_h\in X_h}\frac{a(q_h,\varphi_h)}{\|q_h\|_{L^2(\Omega)}} \quad \text{for all } \varphi_h\in Y_h. \tag{2.16}$$

For $\varphi\in Y$ we can therefore define $\Pi_h\varphi\in Y_h$ as the unique solution of the variational problem

$$a(q_h,\Pi_h\varphi) = a(q_h,\varphi) \quad \text{for all } q_h\in X_h, \tag{2.17}$$

where unique solvability follows from $\dim X_h = \dim Y_h$ and (2.16). The latter also implies, together with (2.8),

$$\|\Pi_h\varphi\|_Y \leq \frac{\sqrt{2}}{c_{Y_h}}\|\varphi\|_Y. \tag{2.18}$$

With this we can prove the discrete stability condition (2.11) via the criteria of Fortin [9], with $c_S = \frac{c_{Y_h}}{\sqrt{2}}$.

It remains to define the finite element test space $Y_h\subset Y$ such that (2.15) is satisfied with a positive constant c_{Y_h} independent of the discretization parameter h.

2.4 Tensor-Product Meshes

Since X_h is defined as the space of piecewise constant basis functions, we find the coefficients $\overline{p}_k = \overline{p}_h|_{\tau_k}$ of $\overline{p}_h\in X_h$ as

$$\overline{p}_k = \frac{1}{|\tau_k|}\int_{\tau_k}[-\Delta\varphi_h(x)]\,dx \quad \text{for } k=1,\dots,N.$$

We first consider the one-dimensional case where the computational domain $\Omega=(0,1)$ is decomposed into N finite elements $\tau_k=(x_{k-1},x_k)$ of mesh size $h=\frac{1}{N}$, i.e., $x_k=kh$ for $k=0,1,\dots,N$. For a finite element $\tau_k=(x_{k-1},x_k)$, $k=1,\dots,N$, the piecewise constant basis function ψ_k is defined as

$$\psi_k(x) = \begin{cases} 1 & \text{for } x\in(x_{k-1},x_k), \\ 0 & \text{else.}\end{cases}$$

For the definition of a conforming test space $Y_h\subset Y$ we use piecewise quadratic B-splines, i.e., for $k=2,\dots,N-1$,

$$\varphi_k(x) = \begin{cases} \frac12\frac{1}{h^2}(x-x_{k-2})^2 & \text{for } x\in[x_{k-2},x_{k-1}], \\ \frac14\frac{1}{h^2}[3h^2-(2x-x_{k-1}-x_k)^2] & \text{for } x\in[x_{k-1},x_k], \\ \frac12\frac{1}{h^2}(x-x_{k+1})^2 & \text{for } x\in[x_k,x_{k+1}], \\ 0 & \text{else,}\end{cases} \tag{2.19}$$

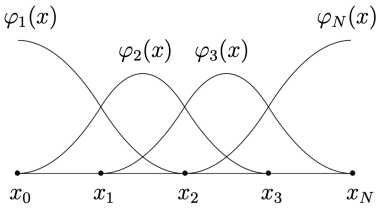

Figure 1: Illustration of the smooth, piecewise quadratic functions used as basis for the one-dimensional test space.

while for $k = 1$ and $k = N$ we use the modified splines

$$\varphi_1(x) = \begin{cases} 1 - \frac{1}{2}\frac{1}{h^2}(x - x_0)^2 & \text{for } x \in [x_0, x_1], \\ \frac{1}{2}\frac{1}{h^2}(x - x_2)^2 & \text{for } x \in [x_1, x_2], \\ 0 & \text{else,} \end{cases} \tag{2.20}$$

and

$$\varphi_N(x) = \begin{cases} \frac{1}{2}\frac{1}{h^2}(x - x_{N-2})^2 & \text{for } x \in [x_{N-2}, x_{N-1}], \\ 1 - \frac{1}{2}\frac{1}{h^2}(x - x_N)^2 & \text{for } x \in [x_{N-1}, x_N], \\ 0 & \text{else,} \end{cases} \tag{2.21}$$

to ensure conformity $Y_h \subset Y$ (see Figure 1). For a given $\varphi_h \in Y_h$ we then conclude $\overline{p}_h = -\varphi_h'' \in X_h$, and hence (2.15) follows with $c_{Y_h} = 1$.

In the multi-dimensional case ($n > 1$), we can define Y_h as the tensor product of the one-dimensional test space. However, in this case it follows that $-\Delta\varphi_h \notin X_h$ is not piecewise constant, i.e., we need to use the L^2 projection $\overline{p}_h = Q_h[-\Delta\varphi_h] \in X_h$, see (2.14).

Example 2.1. For a given mesh size h we consider the computational domain $\Omega = (0, 2h)^2$ which is decomposed into four finite elements τ_k. When using the one-dimensional basis functions

$$\varphi_1(x) = \begin{cases} 1 - \frac{1}{2}\frac{x^2}{h^2} & \text{for } x \in (0, h), \\ \frac{1}{2}\frac{1}{h^2}(x - 2h)^2 & \text{for } x \in (h, 2h), \end{cases}$$

$$\varphi_2(x) = \begin{cases} \frac{1}{2}\frac{x^2}{h^2} & \text{for } x \in (0, h), \\ 1 - \frac{1}{2}\frac{1}{h^2}(x - 2h)^2 & \text{for } x \in (h, 2h), \end{cases}$$

we can write $\varphi_h \in Y_h$ as

$$\varphi_h(x) = a_{11}\varphi_1(x_1)\varphi_1(x_2) + a_{21}\varphi_2(x_1)\varphi_1(x_2) + a_{12}\varphi_1(x_1)\varphi_2(x_2) + a_{22}\varphi_2(x_1)\varphi_2(x_2),$$

for which we compute

$$\|\Delta\varphi_h\|^2_{L^2(\Omega)} = \frac{1}{45}\frac{1}{h^2}\left(\begin{pmatrix} 178 & -88 & -88 & -2 \\ -88 & 178 & -2 & -88 \\ -88 & -2 & 178 & -88 \\ -2 & -88 & -88 & 178 \end{pmatrix}\begin{pmatrix} a_{11} \\ a_{21} \\ a_{12} \\ a_{22} \end{pmatrix}, \begin{pmatrix} a_{11} \\ a_{21} \\ a_{12} \\ a_{22} \end{pmatrix}\right).$$

For the piecewise constant L^2 projection $\overline{p}_h = Q_h[-\Delta\varphi_h] \in X_h$ as defined in (2.14) we obtain

$$\|\overline{p}_h\|^2_{L^2(\Omega)} = \frac{1}{9}\frac{1}{h^2}\left(\begin{pmatrix} 34 & -16 & -16 & -2 \\ -16 & 34 & -2 & -16 \\ -16 & -2 & 34 & -16 \\ -2 & -16 & -16 & 34 \end{pmatrix}\begin{pmatrix} a_{11} \\ a_{21} \\ a_{12} \\ a_{22} \end{pmatrix}, \begin{pmatrix} a_{11} \\ a_{21} \\ a_{12} \\ a_{22} \end{pmatrix}\right).$$

It is easy to check that the eigenvectors of both matrices coincide, i.e.,

$$\underline{v}^1 = \begin{pmatrix} 1 \\ 1 \\ 1 \\ 1 \end{pmatrix}, \quad \underline{v}^2 = \begin{pmatrix} 1 \\ -1 \\ -1 \\ 1 \end{pmatrix}, \quad \underline{v}^3 = \begin{pmatrix} -1 \\ 0 \\ 0 \\ 1 \end{pmatrix}, \quad \underline{v}^4 = \begin{pmatrix} 0 \\ -1 \\ 1 \\ 0 \end{pmatrix},$$

and for all $\underline{a} \in \mathbb{R}^4$ we can write

$$\underline{a} = \sum_{k=1}^{4} a_k \underline{v}^k.$$

With this we compute

$$\|\Delta \varphi_h\|^2 = \frac{1}{45} \frac{1}{h^2} [1408 a_2^2 + 360 a_3^2 + 360 a_4^2]$$

as well as

$$\|\overline{p}_h\|^2_{L^2(\Omega)} = \frac{1}{9} \frac{1}{h^2} [256 a_2^2 + 72 a_3^2 + 72 a_4^2].$$

Hence we conclude

$$\|\overline{p}_h\|^2_{L^2(\Omega)} \geq \frac{10}{11} \|\Delta \varphi_h\|^2_{L^2(\Omega)},$$

which is (2.15) with $c_{Y_h} = \frac{10}{11}$.

While the approach as given in the previous example can be generalized to any tensor product decomposition of Ω, a rigorous proof of (2.15) remains open. Yet our numerical results indicate that (2.15) is satisfied also in more general situations.

2.5 Simplicial Meshes

As we have just seen, considering tensor-product spaces leads to $\Delta \varphi_h \notin X_h$, which requires showing the reverse inequality (2.15). Moreover, tensor-product meshes impose an obviously strong restriction on the geometries that can be discretized. Also notice that the tensor products of one-dimensional H^2 functions are also in $H^2(\Omega)$, which is in some sense more than we need for stability, since $H^2(\Omega) \subseteq H^1_\Delta(\Omega)$. In this context, we can alternatively construct an appropriate test space by taking functions $\varphi_h \in H^1_\Delta(\Omega)$ so that $\Delta \varphi_h = \operatorname{div} \boldsymbol{\psi}_h$, where $\boldsymbol{\psi}_h$ are basis functions from the lowest-order Raviart–Thomas space RT_0. On simplicial meshes (triangles for $n = 2$, tetrahedra for $n = 3$), this space contains piecewise linear, vector-valued functions $\boldsymbol{\psi}_h \in H(\operatorname{div}, \Omega)$. Then, by selecting only the basis functions satisfying the boundary condition $\boldsymbol{\psi}_h \cdot \boldsymbol{n}_x = 0$ on $\partial\Omega$, we will have

$$\Delta \varphi_h = \operatorname{div} \boldsymbol{\psi}_h \in X_h \subset L^2(\Omega),$$

so that stability follows immediately from (2.15) with $c_{Y_h} = 1$. Note that, since the degrees of freedom of the Raviart–Thomas element are the normal components $\boldsymbol{\psi}_h \cdot \boldsymbol{n}_x$ on the element edges ($n = 2$) or faces ($n = 3$), it is straightforward to select only those with zero value on $\partial\Omega$. Formally, for each element τ_k we define the actual scalar test function $\varphi_k \in Y_h \subset Y$ as the unique solution of the Neumann boundary value problem

$$-\Delta \varphi_k = -\operatorname{div} \boldsymbol{\psi}_k \quad \text{in } \Omega, \qquad \partial_n \varphi_k = 0 \quad \text{on } \Gamma, \qquad \int_\Omega \varphi_k \, dx = a_k > 0, \tag{2.22}$$

which gives us, using (2.4),

$$\int_\Omega p_h [-\operatorname{div} \boldsymbol{\psi}_k] \, dx + \frac{a_k}{|\Omega|} \int_\Omega p_h \, dx = \int_\Omega (\boldsymbol{f} + \nu \Delta \boldsymbol{u}) \cdot \nabla \varphi_k \, dx. \tag{2.23}$$

While we can evaluate the left-hand side in (2.23) using only the Raviart–Thomas functions $\boldsymbol{\psi}_k$, computing the right-hand side can be more involved. From (2.22) we conclude the representation

$$\nabla \varphi_k = \boldsymbol{\psi}_k + \operatorname{curl} \boldsymbol{A}$$

for arbitrary vector fields $\boldsymbol{A}$ satisfying $\boldsymbol{n}_x \cdot \operatorname{curl} \boldsymbol{A} = 0$ on Γ. Then

$$\int_\Omega (\boldsymbol{f} + \nu\Delta\boldsymbol{u}) \cdot \nabla\varphi_k \, dx = \int_\Omega (\boldsymbol{f} + \nu\Delta\boldsymbol{u}) \cdot [\boldsymbol{\psi}_k + \operatorname{curl} \boldsymbol{A}] \, dx = \int_\Omega (\boldsymbol{f} + \nu\Delta\boldsymbol{u}) \cdot \boldsymbol{\psi}_k \, dx,$$

provided that

$$\int_\Omega (\boldsymbol{f} + \nu\Delta\boldsymbol{u}) \cdot [\operatorname{curl} \boldsymbol{A}] \, dx = 0$$

for all $\boldsymbol{A}$ with $\boldsymbol{n}_x \cdot \operatorname{curl} \boldsymbol{A} = 0$ on Γ. Indeed, if $\boldsymbol{f} + \nu\Delta\boldsymbol{u} = \nabla\phi$ is a gradient field, we have

$$\begin{aligned}\int_\Omega (\boldsymbol{f} + \nu\Delta\boldsymbol{u}) \cdot [\operatorname{curl} \boldsymbol{A}] \, dx &= \int_\Omega \nabla\phi \cdot [\operatorname{curl} \boldsymbol{A}] \, dx \\ &= \int_\Gamma \phi \boldsymbol{n}_x \cdot [\operatorname{curl} \boldsymbol{A}] \, ds_x - \int_\Omega \phi \operatorname{div}[\operatorname{curl} \boldsymbol{A}] \, dx = 0.\end{aligned}$$

This is exactly the case we have here – as a matter of fact, with $\phi = p$. Therefore, we can work directly with the Raviart–Thomas functions $\boldsymbol{\psi}_k$, without having to actually solve (2.22) for φ_k, which is thus implicitly defined. We finally get

$$\int_\Omega p_h[-\operatorname{div} \boldsymbol{\psi}_k] \, dx + \frac{a_k}{|\Omega|} \int_\Omega p_h \, dx = \int_\Omega (\boldsymbol{f} + \nu\Delta\boldsymbol{u}) \cdot \boldsymbol{\psi}_k \, dx. \tag{2.24}$$

The scaling factor a_k can be chosen either mesh dependent, or simply equal to 1, for example. However, since these test functions do not necessarily form a partition of unity, the scaling $p_h \in L^2_0(\Omega)$ is no longer exactly satisfied. This does not matter in practice, since one can solve for p_h and then simply compute

$$\widetilde{p}_h = p_h - \frac{1}{|\Omega|} \int_\Omega p_h \, dx,$$

which will then have zero mean, by construction.

For an element τ_k, the support of $\boldsymbol{\psi}_k$ will cover no more than $n + 2$ elements: τ_k itself and all adjacent elements with a common face ($n = 3$) or edge ($n = 2$). We then select $\boldsymbol{\psi}_k \in \mathrm{RT}_0$ such that $\boldsymbol{\psi}_k \cdot \boldsymbol{n}_x = 1$ on $\partial\tau_k \setminus \Gamma$, $\boldsymbol{\psi}_k \cdot \boldsymbol{n}_x = -1$ on the common faces ($n = 3$) or edges ($n = 2$) of neighboring elements, and $\boldsymbol{\psi}_k \cdot \boldsymbol{n}_x = 0$ elsewhere. Figure 2 illustrates the setup in two dimensions, and details on the properties and the implementation of Raviart–Thomas functions can be found in [2].

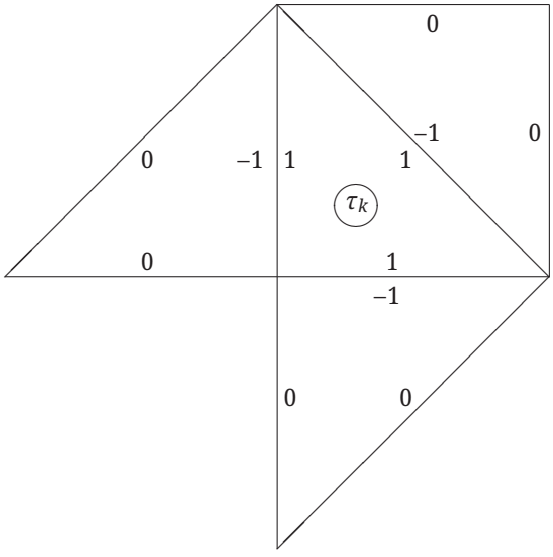

Figure 2: Support of the vector–valued test function $\boldsymbol{\psi}_k \in \mathrm{RT}_0$ and its normal values $\boldsymbol{\psi}_k \cdot \boldsymbol{n}_x$, for an internal element τ_k in two dimensions. The negative values in adjacent elements account for the change in the local definition (direction) of $\boldsymbol{n}_x$.

A limitation of this approach is the need to consider the full second-order term $\Delta \boldsymbol{u}$, since the Raviart–Thomas functions $\boldsymbol{\psi}_k$ are not regular enough to allow further integration by parts. Therefore, when $\boldsymbol{u}$ is replaced by a piecewise linear interpolation $\boldsymbol{u}_h$, the Laplacian will have to be reconstructed using some appropriate technique (see, e.g., [13] for a simple approach). Alternatively, instead of the pressure Poisson equation we can consider a least-squares approach to compute the pressure.

3 A Least-Squares Recovery Method

Instead of (2.1) we now consider the functional

$$\begin{aligned} \mathcal{J}(p) &= \frac{1}{2} \| \nabla p - \boldsymbol{f} - \nu \Delta \boldsymbol{u} \|^2_{H^{-1}(\Omega)} \\ &= \frac{1}{2} \langle A^{-1}(\nabla p - \boldsymbol{f} - \nu \Delta \boldsymbol{u}), \nabla p - \boldsymbol{f} - \nu \Delta \boldsymbol{u} \rangle_\Omega \end{aligned} \tag{3.1}$$

to be minimized, where the vector Laplacian $A : \boldsymbol{H}^1_0(\Omega) \to \boldsymbol{H}^{-1}(\Omega)$ is defined as

$$\langle A \boldsymbol{w}, \boldsymbol{v} \rangle_\Omega = \int_\Omega \nabla \boldsymbol{w} : \nabla \boldsymbol{v} \, dx \quad \text{for all } \boldsymbol{w}, \boldsymbol{v} \in \boldsymbol{H}^1_0(\Omega).$$

The minimizer of (3.1) is then given as the unique solution $p \in L^2_0(\Omega)$ of the gradient equation

$$\langle A^{-1}(\nabla p - \boldsymbol{f} - \nu \Delta \boldsymbol{u}), \nabla q \rangle_\Omega = 0 \quad \text{for all } q \in L^2_0(\Omega). \tag{3.2}$$

By introducing $\boldsymbol{w} = A^{-1}(\nabla p - \boldsymbol{f} - \nu \Delta \boldsymbol{u})$, this is equivalent to a variational formulation to find $\boldsymbol{w} \in \boldsymbol{H}^1_0(\Omega)$ and $p \in L^2(\Omega)$ such that

$$\int_\Omega \nabla \boldsymbol{w} : \nabla \boldsymbol{v} \, dx + \int_\Omega p \operatorname{div} \boldsymbol{v} \, dx = \nu \int_\Omega \nabla \boldsymbol{u} : \nabla \boldsymbol{v} \, dx - \int_\Omega \boldsymbol{f} \cdot \boldsymbol{v} \, dx \tag{3.3}$$

and

$$- \int_\Omega q \operatorname{div} \boldsymbol{w} \, dx + \int_\Omega p \, dx \int_\Omega q \, dx = 0 \tag{3.4}$$

is satisfied for all $\boldsymbol{v} \in \boldsymbol{H}^1_0(\Omega)$ and $q \in L^2(\Omega)$. Note that system (3.3) and (3.4) is also known as Stokes estimator [1, 4]. By construction, we have that $\boldsymbol{w} = \boldsymbol{0}$. For the numerical solution of the Stokes system (3.3) and (3.4) we can use any stable finite element scheme. One possible approach is to consider first the finite element discretization of the gradient equation (3.2) in its stabilized form to find $p \in L^2(\Omega)$ such that

$$\langle A^{-1}(\nabla p - \boldsymbol{f} - \nu \Delta \boldsymbol{u}), \nabla q \rangle_\Omega + \int_\Omega p \, dx \int_\Omega q \, dx = 0 \quad \text{for all } q \in L^2(\Omega). \tag{3.5}$$

Note that (3.5) is the Schur complement equation of the modified Stokes system (3.3) and (3.4). Since the related bilinear form

$$\langle A^{-1} \nabla p, \nabla q \rangle_\Omega + \int_\Omega p \, dx \int_\Omega q \, dx \tag{3.6}$$

is bounded for all $p, q \in L^2(\Omega)$, and elliptic in $L^2(\Omega)$, unique solvability of (3.5) follows. As before, let $X_h \subset L^2(\Omega)$ be the space of piecewise constant basis functions. Then, we consider the Galerkin formulation to find $p_h \in X_h$ such that

$$\langle A^{-1}(\nabla p_h - \boldsymbol{f} - \nu \Delta \boldsymbol{u}), \nabla q_h \rangle_\Omega + \int_\Omega p_h \, dx \int_\Omega q_h \, dx = 0 \quad \text{for all } q_h \in X_h. \tag{3.7}$$

Using standard arguments we then conclude Cea's lemma (2.12), and the error estimate (2.13). However, since the bilinear form (3.6) does not allow a direct evaluation, we need to introduce an approximation of

$$\boldsymbol{w} = A^{-1}(\nabla p - \boldsymbol{f} - \nu \Delta \boldsymbol{u})$$

by some $\boldsymbol{w}_h \in \boldsymbol{Y}_h \subset \boldsymbol{H}_0^1(\Omega)$. Hence we consider the finite element approximation of (3.3) and (3.4) to find $\boldsymbol{w}_h \in \boldsymbol{Y}_h$ and $\widetilde{p}_h \in X_h$ such that

$$\int_\Omega \nabla \boldsymbol{w}_h : \nabla \boldsymbol{v}_h \, dx + \int_\Omega \widetilde{p}_h \operatorname{div} \boldsymbol{v}_h \, dx = \nu \int_\Omega \nabla \boldsymbol{u} : \nabla \boldsymbol{v}_h \, dx - \int_\Omega \boldsymbol{f} \cdot \boldsymbol{v}_h \, dx \tag{3.8}$$

and

$$-\int_\Omega q_h \operatorname{div} \boldsymbol{w}_h \, dx + \int_\Omega \widetilde{p}_h \, dx \int_\Omega q_h \, dx = 0 \tag{3.9}$$

is satisfied for all $\boldsymbol{v}_h \in \boldsymbol{Y}_h$ and $q_h \in X_h$. The discrete Schur complement system of (3.8) and (3.9) then defines an approximation of the continuous Schur complement equation (3.7), which can be analyzed via the Strang lemma [5, 18]. To ensure discrete ellipticity of the approximated Schur complement operator, we must define the finite element space $\boldsymbol{Y}_h$ appropriately. An example of velocity discretization that is stable when combined with piecewise constant pressure are continuous, Lagrangian spaces of polynomial degree n (the spatial dimension). Another possible choice is to consider piecewise linear, continuous basis functions defined on a fine enough mesh when compared to the mesh size of X_h. Either way, the order of convergence given in (2.13) will not change.

While we have $\boldsymbol{w} = \boldsymbol{0}$ for the solution of (3.3) and (3.4), this is not true for the discrete counterpart $\boldsymbol{w}_h$. Instead, we may use $\boldsymbol{w}_h$ to define an error indicator to control the finite element error $\|p - \widetilde{p}_h\|_{L^2(\Omega)}$. This follows the general approach as analyzed in [12], and will be discussed in more detail in an upcoming work [14].

4 Numerical Results

This section presents numerical results supporting our a priori estimates. The discrete pressure is piecewise constant, which in the least-squares (LS) case is paired with a piecewise quadratic artificial velocity $\boldsymbol{w}_h$, for inf-sup stability. As done in applications, we will replace $\boldsymbol{u}$ by a first-order interpolation $\boldsymbol{u}_h$, on the same triangulation used for p_h. This allows a simple evaluation of the velocity term $\int_\Gamma (\operatorname{curl} \boldsymbol{u}_h) \cdot (\boldsymbol{n}_x \times \nabla \varphi) \, ds_x$. For the approach using Raviart–Thomas functions, however, a piecewise linear $\boldsymbol{u}_h$ cannot be used, as discussed in Section 2.5. Therefore, in this case we consider a piecewise constant approximation of the Laplacian $\Delta \boldsymbol{u}$.

Consider the computational domain $\Omega = (0,1)^2$, zero right-hand side ($\boldsymbol{f} = \boldsymbol{0}$), $\nu = 1$, and the exact solution given by

$$\boldsymbol{u}(x,y) = \begin{pmatrix} 2y^3 - y \\ 2x^3 - x \end{pmatrix}, \quad p(x,y) = 12xy - 3.$$

We use two families of meshes with the same resolution: one with square elements (for the PPE with spline test functions), and one with triangles (for both the LS and the PPE with Raviart–Thomas functions). The coarsest level is shown in Figure 3, after which several uniform refinements are applied. The relative $L^2(\Omega)$ pressure errors are shown in Table 1, confirming linear convergence for all recovery techniques.

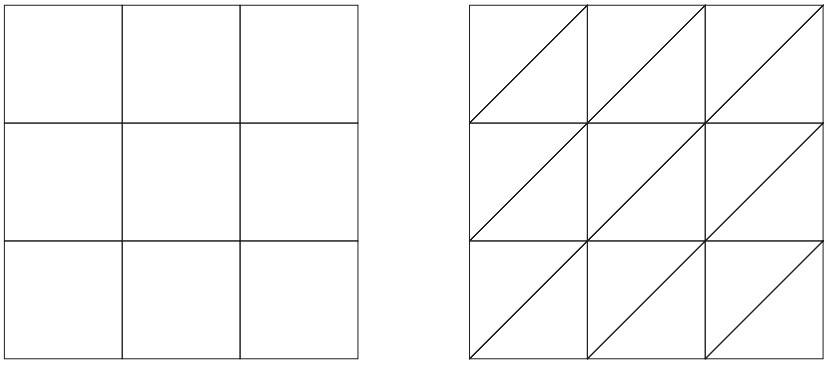

Figure 3: Meshes used as starting point for the refinement study.

	Tensor-product PPE		Simplicial PPE		Simplicial LS	
Refinement level	L^2-error	eoc	L^2-error	eoc	L^2-error	eoc
0	5.20e-1		3.29e-1		4.40e-1	
1	2.77e-1	0.90	1.70e-1	0.95	2.02e-1	1.12
2	1.42e-1	0.96	8.52e-2	0.99	9.25e-2	1.12
3	7.21e-2	0.98	4.26e-2	1.00	4.40e-2	1.07
4	3.62e-2	0.99	2.13e-2	1.00	2.16e-2	1.03
5	1.82e-2	1.00	1.07e-2	1.00	1.07e-2	1.01
6	9.09e-3	1.00	5.33e-3	1.00	5.34e-3	1.00
7	4.55e-3	1.00	2.67e-3	1.00	2.67e-3	1.00

Table 1: Numerical test case confirming the linear convergence of both PPE and LS approaches, using a piecewise constant pressure approximation.

5 Conclusions

In this work, we have presented, analyzed and discretized two distinct pressure recovery methods. The first is an ultra-weak variational formulation for the pressure Poisson equation (PPE). Differently from common approaches, we do not rely on a discontinuous Galerkin framework, nor do we recast the Poisson problem into a mixed first-order system, but rather consider a scalar Galerkin–Petrov formulation. To that end, we use integration by parts to get rid of all derivatives on the trial functions p, which allows us to consider $p \in L^2(\Omega)$ as in the Navier–Stokes system. As a trade-off, we must have H^1 test functions with square-integrable Laplacian, hence the Galerkin–Petrov nature of our framework. When considering these different trial and test spaces, unique solvability of the continuous problem is guaranteed by an inf-sup stability condition. We have then also proved discrete stability and a priori error estimates for a conforming, yet abstract choice of spaces fulfilling certain conditions. When considering piecewise constant trial functions, we have presented a realization of the test space using modified second-order B-splines. In that case, the discrete inf-sup condition is proven in one dimension, while an extension to higher dimensions is sketched. For simplicial meshes, we have also presented an approach using test functions whose divergence is in the lowest-order Raviart–Thomas space.

As an alternative framework requiring only standard Lagrangian finite element spaces, we have also considered a least-squares method that is solved as a Stokes system with artificial velocity. The method results in considerably more degrees of freedom than the PPE, but can be discretized in a much simpler way. Both approaches require the same regularity on the unknown pressure and the velocity data, and also converge with the same order. Although we have considered incompressible velocities here, compressible ones can also be used, since both the ultra-weak PPE and the least-squares approach use test functions with enough regularity to handle the additional terms that appear in the compressible form of the Navier–Stokes equations.

An open problem is extending the ultra-weak discretization to higher-order trial spaces. In fact, first numerical experiments combining piecewise (bi-)linear *ansatz* with Hermite or Argyris polynomials as test functions indicate promising results [16].

Acknowledgment: Part of the work was done when the first author was a PhD student at TU Graz within the lead-project: Mechanics, Modeling, and Simulation of Aortic Dissection.

Funding: The authors acknowledge Graz University of Technology for the financial support.

Note 2: The bibliography has been cross-checked and updated with MathSciNet. Since entries may be mismatched and replaced by a wrong entry (especially: preprints, theses, and translations), please carefully double-check *each* entry.

References

[1] R. Araya, C. Bertoglio, C. Carcamo, D. Nolte and S. Uribe, Convergence analysis of pressure reconstruction methods from discrete velocities, *ESAIM Math. Model. Numer. Anal.* **57** (2023), no. 3, 1839–1861.

[2] C. Bahriawati and C. Carstensen, Three MATLAB implementations of the lowest-order Raviart–Thomas MFEM with a posteriori error control, *Comput. Methods Appl. Math.* **5** (2005), no. 4, 333–361.

[3] M. Berggren, Approximations of very weak solutions to boundary-value problems, *SIAM J. Numer. Anal.* **42** (2004), no. 2, 860–877.
[4] C. Bertoglio, R. Nuñez, F. Galarce, D. Nordsletten and A. Osses, Relative pressure estimation from velocity measurements in blood flows: State-of-the-art and new approaches, *Int. J. Numer. Methods Biomed. Eng.* **34** (2018), no. 2, Article ID e2925.
[5] S. C. Brenner and L. R. Scott, *The Mathematical Theory of Finite Element Methods*, 3rd ed., Texts Appl. Math. 15, Springer, New York, 2008.
[6] J. A. Burns, T. Lin and L. G. Stanley, A Petrov Galerkin finite-element method for interface problems arising in sensitivity computations, *Comput. Math. Appl.* **49** (2005), no. 11–12, 1889–1903.
[7] A. Ern and J.-L. Guermond, *Theory and Practice of Finite Elements*, Appl. Math. Sci. 159, Springer, New York, 2004.
[8] A. Ern, M. Vohralík and M. Zakerzadeh, Guaranteed and robust L^2-norm *a posteriori* error estimates for 1D linear advection problems, *ESAIM Math. Model. Numer. Anal.* **55** (2021), S447–S474.
[9] M. Fortin, An analysis of the convergence of mixed finite element methods, *RAIRO Anal. Numér.* **11** (1977), no. 4, 341–354.
[10] J. Henning, D. Palitta, V. Simoncini and K. Urban, An ultraweak space-time variational formulation for the wave equation: Analysis and efficient numerical solution, *ESAIM Math. Model. Numer. Anal.* **56** (2022), no. 4, 1173–1198.
[11] H. Johnston and J.-G. Liu, Accurate, stable and efficient Navier–Stokes solvers based on explicit treatment of the pressure term, *J. Comput. Phys.* **199** (2004), no. 1, 221–259.
[12] C. Köthe, R. Löscher and O. Steinbach, Adaptive least-squares space-time finite element methods, preprint (2023), https://arxiv.org/abs/2309.14300.
[13] J. Li and J. Ying, A stabilized finite volume element method for solving Poisson–Nernst–Planck equations, *Int. J. Numer. Methods Biomed. Eng.* **38** (2022), no. 1, Paper No. e3543.
[14] R. Löscher, D. R. Q. Pacheco and O. Steinbach, An adaptive least-squares finite element method for the pressure reconstruction in fluid mechanics, in preparation (2023).
[15] D. Nolte, J. Urbina, J. Sotelo, L. Sok, C. Montalba, I. Valverde, A. Osses, S. Uribe and C. Bertoglio, Validation of 4D flow based relative pressure maps in aortic flows, *Med. Image Anal.* **74** (2021), Article ID 102195.
[16] D. R. Q. Pacheco, *Stable and Stabilised Finite Element Methods for Incompressible Flows of Generalised Newtonian Fluids*, Computation Eng. Sci. 42, Technischen Universität Graz, Graz, 2021.
[17] R. L. Sani, J. Shen, O. Pironneau and P. M. Gresho, Pressure boundary condition for the time-dependent incompressible Navier–Stokes equations, *Internat. J. Numer. Methods Fluids* **50** (2006), no. 6, 673–682.
[18] O. Steinbach, *Numerical Approximation Methods for Elliptic Boundary Value Problems*, Springer, New York, 2008.